
Cooperative α -helix unfolding in a protein–DNA complex from hydrogen–deuterium exchange

ROBERTO K. SALINAS,¹ TAMMO DIERCKS, ROBERT KAPTEIN, AND ROLF BOELEN

Bijvoet Center for Biomolecular Research, Utrecht University, 3584 CH Utrecht, The Netherlands

(RECEIVED November 1, 2005; FINAL REVISION February 16, 2006; ACCEPTED March 7, 2006)

Abstract

We present experimental evidence for a cooperative unfolding transition of an α -helix in the lac repressor headpiece bound to a symmetric variant of the *lac* operator, as inferred from hydrogen–deuterium (H–D) exchange experiments monitored by NMR spectroscopy. In the EX1 limit, observed exchange rates become pH-independent and exclusively sensitive to local structure fluctuations that expose the amide proton H^N to exchange. Close to this regime, we measured decay rates of individual backbone H^N signals in D_2O , and of their mutual H^N – H^N NOE by time-resolved two-dimensional (2D) NMR experiments. The data revealed correlated exchange at the center of the lac headpiece recognition helix, Val20–Val23, and suggested that the correlation breaks down at Val24, at the C terminus of the helix. A lower degree of correlation was observed for the exchange of Val9 and Ala10 at the center of helix 1, while no correlation was observed for Val38 and Glu39 at the center of helix 3. We conclude that H^N exchange in the recognition helix and, to some extent, in helix 1 is a cooperative event involving the unfolding of these helices, whereas the H^N exchange in helix 3 is dominated by random local structure fluctuations.

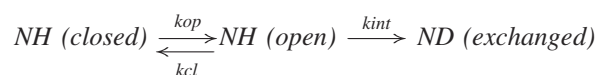
Keywords: hydrogen–deuterium exchange; folding; cooperativity; protein–DNA complex; Lac repressor

Supplemental material: see www.proteinscience.org

The protection of amide protons, H^N , against exchange with the solvent is associated with their participation in hydrogen bonds and exposure to the solvent (for recent reviews, see Englander 2000; Dempsey 2001; Myers and Oas 2002). Although there is no consensus on what degree of protection against exchange indicates hydrogen bonding, slow H^N exchange rates are often observed within secondary structure elements.

H^N exchange in proteins is generally explained by a model in which structural fluctuations convert the amide

proton from an exchange-protected (closed) state to an exchange-competent (open) state, as described by the following scheme (Berger and Linderstrøm-Lang 1957; Hvidt and Nielsen 1966; Englander et al. 1997):



where k_{op} and k_{cl} are the kinetic rates for the opening and closing reactions, respectively, and k_{int} is the intrinsic rate of exchange for the unprotected amide. Once in the open state, exchange either occurs by an acid-catalyzed reaction below $pH \approx 4$, or by a base-catalyzed reaction at higher pH (Woodward et al. 1982; Englander and Kaltenbach 1983). This reaction has a distinct, pH-dependent rate constant k_{int} for each backbone amide, which can be predicted accurately (Bai et al. 1993).

¹Present address: Department of Biochemistry, Institute of Chemistry, University of São Paulo, São Paulo SP, 05513-970, Brazil.

Reprint requests to: Rolf Boelens, Department of NMR Spectroscopy, Bijvoet Center for Biomolecular Research, Utrecht University, Padualaan 8, 3584 CH Utrecht, The Netherlands; e-mail: r.boelens@chem.uu.nl; fax: +31-30-253-7623.

Article published online ahead of print. Article and publication date are at <http://www.proteinscience.org/cgi/doi/10.1110/ps.051938006>.

The general two-state model has two limiting regimes, EX1 and EX2. In the EX1 limit, k_{int} is much larger than k_{cl} , the rate constant of the competing closing reaction, and every H^{N} reaching the open state will immediately exchange with the solvent. The observed rate, k_{obs} , then becomes equal to k_{op} , and the EX1 regime is therefore characterized by a disappearance of the pH dependence for k_{obs} :

$$k_{\text{obs}} = k_{\text{op}}$$

Conversely, in the EX2 regime, k_{cl} is larger than k_{int} , and k_{obs} through the latter here retains a pronounced pH dependence:

$$k_{\text{obs}} = \frac{k_{\text{op}}}{k_{\text{cl}}} k_{\text{int}}$$

The system can be pushed into the EX1 regime, e.g., by increasing k_{int} relative to k_{cl} through an increase in the pH, or by decreasing k_{cl} through addition of denaturants (see, for example, Sivaraman et al. 2001; Qu and Bolen 2003). This regime is characterized by a disappearance of the pH dependence for k_{obs} , which then directly reflects the rate k_{op} for underlying structural opening motions. In contrast, in the EX2 limit we can derive the free energy ΔG_{op}^0 for the opening and closing reactions, after prediction of k_{int} (Bai et al. 1993):

$$\Delta G_{\text{op}}^0 = -RT \ln \left[\frac{k_{\text{op}}}{k_{\text{cl}}} \right] = -RT \ln \left[\frac{k_{\text{obs}}}{k_{\text{int}}} \right]$$

Measurements of H–D exchange in both the EX1 and EX2 regimes therefore yield valuable thermodynamic and kinetic information for individual residues. It is an established technique to study protein folding and unfolding pathways, protein stability, dynamics, protein–DNA interactions, and allosteric changes (Englander et al. 1992; Mayo and Baldwin 1993; Bai et al. 1995; Englander 2000; Kalodimos et al. 2002; Luque et al. 2002; Ferraro et al. 2004).

Two types of structural fluctuations may lead to the open state and, thus, exposure of an H^{N} to exchange with the solvent (Woodward et al. 1982; Englander and Kallenbach 1983). For one, local structural fluctuations and temporary breaks of hydrogen bonds may occur without correlation, as proposed in penetration models where the solvent accesses the protein's interior through channels or cavities formed by transient local structure changes (Woodward et al. 1982). For another, local structure fluctuations may occur in a correlated way, as in cooperative transient unfolding of segments of second-

ary structure. Correlation in these underlying opening motions then leads to correlation for the observed H–D exchange. Approaching the EX1 limit to maximize the sensitivity of the observable k_{obs} on these opening motions (see k_{op}), therefore, is a prerequisite for studies on the degree of correlation between the H–D exchange of neighboring amide protons. While local or global unfolding processes were shown to be involved in the mechanism of H–D exchange in various systems (Kim and Woodward 1993; Mayo and Baldwin 1993; Bai et al. 1995; Loh et al. 1996; Sivaraman et al. 2001; Qu and Bolen 2003), correlated exchange of neighboring H^{N} has rarely been demonstrated experimentally (Wagner 1980; Roder et al. 1985; Pinheiro et al. 2000; Uchida et al. 2005).

Here we report a study on the correlated nature of H–D exchange of amide protons in the DNA-binding domain of the lac repressor, the so-called lac headpiece, in complex with a symmetric *lac* operator, lac-SymL. Previous H–D exchange studies on this complex have shown that amino acids from the various α -helices can be grouped according to their opening rates (Kalodimos et al. 2002). We now focus on the amide protons within the slowest exchanging core of the complex, for which we have measured H–D exchange rates and exchange decay rates of mutual H^{N} – H^{N} NOE cross-peaks in the EX1 regime. The data reveal that NOE decay rates are similar to individual H–D exchange rates for the H^{N} of Val20 to Val23 at the center of the recognition helix, indicating that their exchange is correlated. A somewhat lower degree of correlation was observed for the exchange of Ala13 and Val15 in the β -turn of the helix–turn–helix motif and for the exchange of Val9 and Ala10 at the center of helix 1, while no correlation was observed for Val38 and Glu39 at the center of helix 3. We therefore propose that, under the conditions of high pH, H–D exchange of backbone H^{N} at the center of the recognition helix occurs in one event, a reversible cooperative unfolding process on a timescale of ~ 1 d. In contrast, uncorrelated local structure fluctuations contribute to the exchange mechanism in helix 1 and the adjacent β -turn and dominate H–D exchange in helix 3.

Results

We have measured H–D exchange rates on the protein–DNA complex of the dimeric lac headpiece (residues 1–62 of lac repressor) and the lac-SymL operator. Mutation of Val52 to a cysteine (V52C) enabled covalent dimerization of the lac headpiece through oxidation of the introduced Cys52 (Kalodimos et al. 2001). The lac-SymL operator is a palindrome of the left side of the natural *lac* operator O1 and lacks the central GC base pair (Sadler et al. 1983; Simons et al. 1984); it forms a very

stable complex with the lac headpiece (Kalodimos et al. 2001).

As described previously (Wagner 1980, 1983; Boelens et al. 1985; Roder et al. 1985), correlated or random H–D exchange of two amide protons can be distinguished by the decay rate of their mutual NOE. The local structure fluctuations preceding H–D exchange may thereby be either uncorrelated or correlated. In the EX2 regime, however, any initial correlation quickly vanishes since individual amide protons can interconvert randomly between open and closed states several times before the slower deuterium exchange occurs. It is therefore necessary to ensure that individual amide protons exchange according to the EX1 mechanism, where every H^N reaching the open state will immediately exchange with the solvent. It is well accepted that at high pH the amide exchange reaches this EX1 condition (Hvidt and Nielsen 1966; Englander 2000), a condition that can be tested (Qu and Bolen 2003). Previously, we noted that the amide proton exchange of the helical residues of the lac repressor headpiece complexed to DNA became pH independent at high pH values (Kalodimos et al. 2002). For this reason, we performed all experiments at a high pH = 9.5, close to the plateau value for k_{obs} . Importantly, the lack of any significant changes in either 1H – ^{15}N HSQC or NOESY spectrum proved that the complex remained stable under these experimental conditions.

Exchange rates of individual amides

We monitored H–D exchange of backbone H^N for Val9 and Ala10 at the center of the helix 1; Ala13 and Val15 in the β -turn; Val20, Ser21, Arg22, Val23, and Val24 in the recognition helix; and Val 38 and Glu 39 at the center of helix 3 (Fig. 1). Observed exchange rates, k_{obs} , and calculated intrinsic rates, k_{int} , at pH 9.5 are summarized in Table 1. Except for the H^N of Ala13 and Val15, these backbone amide protons lie within the slowly exchanging core of the protein and have opening rates on the order of 10^{-5} sec^{-1} (Kalodimos et al. 2002). While exchange rates range from 1 to $3 \times 10^{-5} \text{ sec}^{-1}$ within the first and the recognition helices (Table 1), the H^N of Val38 and Glu39 in helix 3 exchange typically two to three times faster, and the H^N of Ala13 and Val15 in the β -turn exchange typically six times faster.

The k_{int} rates of individual unprotected amide protons, on the other hand, vary by more than a factor of 10, ranging from $0.07 \times 10^4 \text{ sec}^{-1}$ for Val9 to $1.35 \times 10^4 \text{ sec}^{-1}$ for Arg22 (Table 1). The slightly faster H–D exchange rates observed at the center of helix 3 and in the β -turn between the first and the recognition helices could be attributed to their increased solvent exposure; moreover, neither helix 3 nor the β -turn is stabilized by protein–DNA contacts. A closer inspection of the data

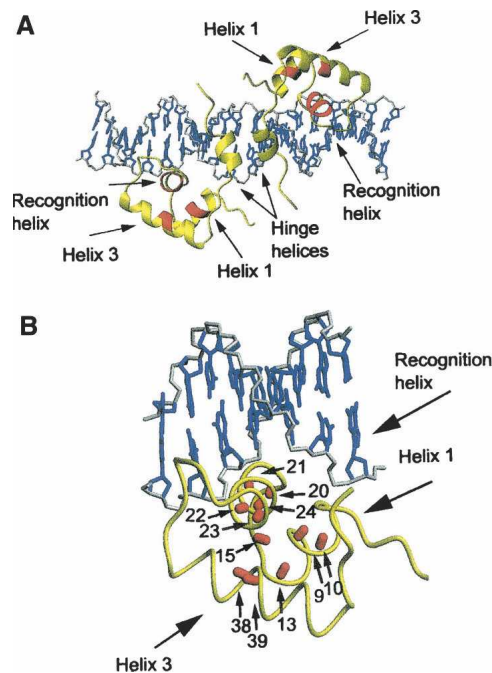


Figure 1. (A) NMR structure of lac headpiece (residues 1–62 of lac repressor) bound to lac operator SymL (PDB 1CJG). The three α -helices—helix 1 (residues 5–13), recognition helix (residues 17–25), and helix 3 (residues 32–45)—are indicated. The first two helices form a helix–turn–helix (HTH) motif packed against helix 3 to form a globular domain. Residues in the N-terminal part of helix 1 and in the recognition helix participate in important protein–DNA contacts with the DNA major groove. (B) Indication of the amide groups for which H–D exchange was monitored (red cylinders). Only one monomer bound to a half operator is shown, since the structure of the protein–DNA complex is symmetric.

(Table 1) shows that differences in k_{int} and k_{obs} do not correlate for the various H^N , further indicating that these protons exchange near the EX1 regime where k_{obs} is independent of k_{int} .

Decay rates of H^N – H^N NOEs

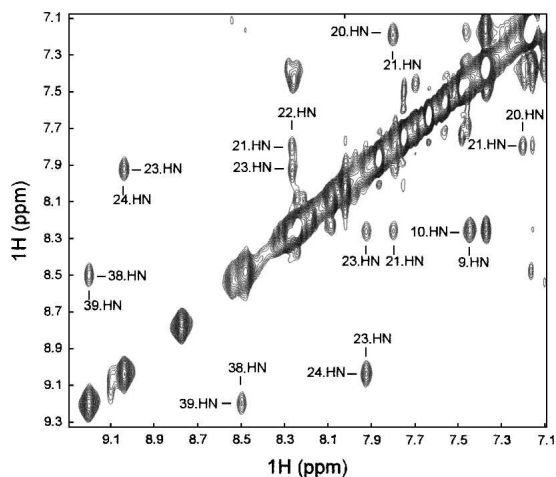
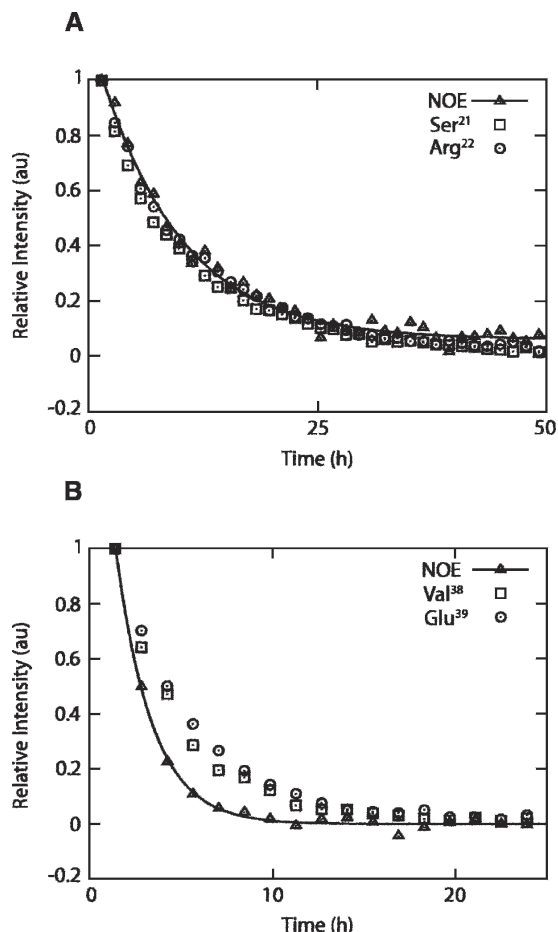
In order to investigate whether the H–D exchange of neighboring amide protons is correlated, we compared decay rates of sequential H^N – H^N NOE cross-peaks with those of individual amide protons in the ^{15}N –HSQC. The almost instantaneous H–D exchange of most amide protons greatly facilitated identification of nonoverlapping sequential H^N – H^N NOE cross-peaks for the slowly exchanging Val9–Ala10, Ala13–Val15, Val20–Ser21, Ser21–Arg22, Arg22–Val23, Val23–Val24, and Val38–Glu39 pairs (Fig. 2). Figure 3 shows two example curves of the H–D exchange decay for sequential NOE cross-peaks and corresponding individual ^{15}N –HSQC peaks, while Table 2 lists the exchange decay rates derived for all relevant NOE signals by single exponential fitting.

Table 1. Observed (k_{obs}) and intrinsic (k_{int}) H–D exchange rates of amide protons within helix I and recognition helix, measured at pH 9.5 and T = 308.5 K

H ^N	k_{obs} (10^{-5} sec ⁻¹)	k_{int} (10^4 sec ⁻¹)
Helix I		
Val9	0.99 ± 0.03	0.07
Ala10	1.53 ± 0.02	0.41
β -turn		
Ala13	15.84 ± 0.02	0.63
Val15	12.56 ± 0.01	0.17
Recognition helix		
Val20	2.00 ± 0.02	0.18
Ser21	3.00 ± 0.06	0.95
Arg22	2.71 ± 0.05	1.35
Val23	1.78 ± 0.03	0.19
Val24	3.15 ± 0.05	0.081
Helix III		
Val38	7.99 ± 0.13	0.15
Glu39	6.80 ± 0.08	0.13

Supplemental Figure S1 shows all H–D exchange decays and their best fits.

If H–D exchange is uncorrelated, the exchange-decay rate k_{NOE} of the NOE between two amide protons H^N₁ and H^N₂ will be equal to the sum of their individual exchange rates k_1 and k_2 (Wagner 1980; Boelens et al. 1985; Roder et al. 1985). In contrast, if exchange is perfectly correlated, both the individual amides and their mutual NOE will exchange-decay with the same rate, $k_1 = k_2 = k_{NOE}$ (Wagner 1980; Boelens et al. 1985; Roder et al. 1985). In order to identify intermediate cases, a measure of correlation was defined (Boelens et al. 1985; Roder et al. 1985) and modified as follows:

**Figure 2.** Expansion of the amide proton region of the first 2D NOE spectrum acquired after dissolution in D₂O. The NOE cross-peaks followed during the course of the experiment are indicated.**Figure 3.** Representative signal decay for neighboring H^N protons (in ¹⁵N-HSQC spectra) and their mutual NOE (in 2D NOE spectra), with a single exponential curve fit indicated. (A) An example of correlated exchange with the decay of the intensity of the amide protons of Ser21 and Arg22, and of their NOE. (B) An example of uncorrelated exchange with the decay of the intensity of the amide protons of Val38 and Arg39, and of their NOE.

$$C_{corr} = \frac{k_1 + k_2 - k_{NOE}}{0.5(k_1 + k_2)}$$

$C_{corr} = 1$ indicates fully correlated exchange, while $C_{corr} = 0$ is expected for uncorrelated H–D exchange.

Figure 3 and Table 2 illustrate that the H^N of Val38 and Glu39 at the center of helix 3 have similar exchange rates, ~ 8 and 7×10^{-5} sec⁻¹, respectively (Table 1). This congruence alone, however, is not enough to prove correlation; rather, the exchange-decay rate of their mutual NOE approaches the sum of the individual H–D exchange rates, and C_{corr} consequently drops to almost zero (Table 2). In contrast, the H^N of Val20 and Ser21 that likewise exchange with similar rates, 2×10^{-5} and 3×10^{-5} sec⁻¹, respectively (Table 1), display perfect correlation with $C_{corr} = 1$ (Table 2). The sequential H^N–H^N

Table 2. Exchange decay rates (k_{NOE}) of H^N – H^N NOE cross-peaks and correlation factors for H–D exchange (C_{corr}), measured at pH 9.5 and $T = 308.5\text{ K}$

HN ₁ –HN ₂	k_{NOE} (10^{-5} sec^{-1}) ^a	C_{corr} ^b
Helix I		
Val9–Ala10	1.94 ± 0.05	0.46 ± 0.04
β-turn		
Ala13–Val15	17.5 ± 3.2	0.77 ± 0.22
Recognition helix		
Val20–Ser21	2.51 ± 0.07	1.00 ± 0.03
Ser21–Arg22	3.13 ± 0.14	0.90 ± 0.05
Arg22–Val23	2.97 ± 0.14	0.68 ± 0.06
Val23–Val24	3.81 ± 0.12	0.45 ± 0.05
Helix III		
Val38–Glu39	14.3 ± 0.5	0.07 ± 0.07

^a k_{NOE} is averaged over both rates obtained for corresponding NOE peaks above and below the diagonal, except for Ala13–Val15 in the β-turn.

^b $C_{\text{corr}} = \frac{k_1+k_2-k_{\text{NOE}}}{0.5(k_1+k_2)}$; errors were obtained from rate errors using standard error propagation.

NOEs in the region between Val21 and Val23 decay with rates comparable to either k_1 or k_2 , indicating a high degree of correlation within the recognition helix (Tables 1, 2). Correlation is maximal for the residue pairs Val20–Ser21 and Ser21–Arg22, with C_{corr} values of 1.00 and 0.90, respectively (Table 2), and decreases toward the C terminus of the recognition helix (at Asp 25). The low $C_{\text{corr}} = 0.45$ observed for the H–D exchange of the Val23 and Val24 amide protons suggests that here correlation breaks down. Analysis of the data for the other segments shows high correlation ($C_{\text{corr}} \sim 0.8$) of H–D exchange for Ala13 and Val15 within the β-turn, whereas moderate correlation of 0.5 was found for Ala9 and Val10 in helix 1.

Two nonsequential H^N – H^N NOE cross-peaks were also observed within the recognition helix. The NOE between Ser21 and Val23 displayed complete correlation ($C_{\text{corr}} = 1.05 \pm 0.22$), corroborating the conclusion that here H–D exchange proceeds by a cooperative mechanism comprising several residues. In contrast, the exchange of Arg22 and Val24 has a negative $C_{\text{corr}} = -0.42 \pm 0.03$ produced by a k_{NOE} much larger than the H–D exchange rates of the individual H^N . This could indicate some spin diffusion contributions for this longer-range NOE, further decreasing the low correlation for the H–D exchange.

Discussion

In this study on the lac headpiece bound to lac-SymL DNA we have used time-resolved 2D NMR spectroscopy to identify correlation of amide proton H–D exchange in the EX1 regime. Such correlated H–D exchange has rarely been observed. For instance, 1D difference NOE

NMR on a partially exchanged sample (Wagner 1980; Roder et al. 1985) indicated correlated exchange in the central part of an antiparallel β-sheet in the bovine pancreatic trypsin inhibitor (BPTI), and H–D exchange monitored by mass spectroscopy revealed correlated exchange in lysozyme (Miranker et al. 1993), in the native turkey ovomucoid third domain (Arrington et al. 1999; Arrington and Robertson 2000) and in cytochrome *c* associated with negatively charged lipid membranes (Pinheiro et al. 2000). Recently, Uchida et al. (2005) reported an elegant method based on the observation of H/D isotope effects from neighboring amide hydrogens on the carbonyl ^{13}C chemical shift to detect correlated exchange, and applied it to the *Streptomyces* subtilisin inhibitor (SSI). In this method, the correlated exchange effects can be directly observed in 1D NMR spectra. Theoretically this could lead to a fast time resolution. However, a practical drawback is that the approach is based on direct ^{13}C detection and that it makes use of small isotope shifts that are only resolved at low NMR fields. These factors make the method rather insensitive. The decay of the NOE intensities for observing correlated exchange of neighboring amide protons, as we used here, can be detected by sensitive ^1H NMR such as at 900 MHz. In principle, this decay could be observed via 1D NMR methods, but in practice it requires 2D NOE spectra, which limits the time resolution for observing the NOE decays to ~ 10 min.

The stability of the free protein is significantly lower than that of the headpiece in the DNA complex, as can be concluded from NMR H–D exchange and thermodynamic studies of the free lac headpiece (Boelens et al. 1985; Felitsky and Record 2003) when compared to data for the bound form (Kalodimos et al. 2002). In free headpiece, the amide exchange rates of the recognition helix are faster than that of helices 1 and 3. In the DNA complex, we observe that the amide exchange of helices 1 and 2 is slower than that of helix 3 and much slower than that of the hinge helix (helix 4). The remarkable stability of the helix–turn–helix motif in the DNA complex is probably due to a close complementary fit between the protein–DNA surfaces and a large number of stabilizing interactions. Our results show that H–D exchange at the center of the recognition helix of the lac headpiece bound to DNA occurs as a single, highly cooperative event. Partial correlation with $C_{\text{corr}} = 0.5$ was observed for the H–D exchange of Val9 and Ala10 at the center of helix 1, suggesting equivalent contributions of uncorrelated and cooperative underlying opening processes. Cooperativity is also observed for Ala13 and Val15 in the β-turn ($C_{\text{corr}} = 0.8$), although these amides exchange faster than those of helices 1 and 2. In contrast, fully uncorrelated local structure fluctuations dominate H–D exchange in helix 3, where C_{corr} for Val38–Glu39 was found to be nearly zero.

This all fits a model in which exchange occurs while the protein is still bound to the DNA, and in which the helices unfold one by one, as concluded before (Kalodimos et al. 2002). When the last two helices finally unfold and the protein dissociates from the DNA, all amide protons exchange, almost in a single event. Whether the unfolding precedes the dissociation of the recognition helix or vice versa cannot be concluded from our data.

Low k_{obs} rates (1.8×10^{-5} – 3.0×10^{-5} sec $^{-1}$) and a high degree of correlation of H–D exchange ($C_{\text{corr}} = 1.0$ – 0.45) observed for Val20, Ser21, Arg22, Val23, and Val24 support the conclusion that they form the stable core of the recognition helix, where the cooperativity of local structural fluctuations decreases toward the C terminus of the helix (at Asn25). Any correlation of local opening motions must vanish at both termini of the helix (Asn25; Tyr17–Thr19) where H–D exchange was too fast even for observation of any H^N signal. This is suggestive of much faster and largely uncorrelated structure fluctuations, such as in helix fraying. The observed loss of cooperativity toward the C terminus may also be related to the nature of helix-to-coil transitions in polypeptides (Zimm and Bragg 1959; Cantor and Schimmel 1980; Qian and Schellman 1992), and is consistent with measurements of $^3J_{\text{NCO}}$ scalar couplings across H-bonds in a polypeptide as a function of TFE concentration that demonstrated the start of H-bond formation at the center of an α -helix (Jaravine et al. 2001).

In conclusion, the high stability of the lac headpiece DNA complex allowed us to study amide proton exchange of individual amide protons under EX1 conditions. Under these conditions, the decay of the NOE between neighboring amide protons due to exchange with deuterium unambiguously registers the correlation in amide proton exchange. Our results indicate strong correlation in the recognition helix of the lac repressor, whereas in helix 1, the exchange of the individual amide protons was only partially correlated and completely uncorrelated in helix 3. The differences in correlations and in opening rates in the three helices of the lac repressor headpiece can be attributed to differences in folding cooperativity that can exist in different secondary structure elements. In this way, our experimental data reconcile different observations of fully uncorrelated amide proton exchange leading to models emphasizing amide proton exchange via solvent penetration and observations of correlated amide proton exchange emphasizing cooperative local structure fluctuations (Miller and Dill 1995). The NMR experiment provides a unique handle to test such kinetic models.

Although the observed unfolding of the individual lac repressor secondary structure elements agrees with a general two-step model for hydrogen exchange under destabilizing conditions (Miller and Dill 1995; Loh et al. 1996), the stabilities of the three helices were not the

same. In fact, the observation of correlated H–D exchange in the recognition helix of the lac headpiece, with different stabilities and cooperativities of the other helices, supports the model for protein–DNA dissociation by a hierarchical process of partial protein unfolding events as suggested earlier (Kalodimos et al. 2002).

Materials and methods

Sample preparation

The V52C mutant lac headpiece (HP62 V52C) was overexpressed in *Escherichia coli* strain DH9 (Hare and Sadler 1978) using a T7 RNA polymerase/promoter system based on the plasmids pET3a and pGP1-2. Expression of RNA polymerase is under control of a P_L promoter and the heat-sensitive cI repressor (cI 857) from phage λ (Tabor and Richardson 1985). Uniformly ^{15}N -labeled protein was grown in Bioexpress (CIL) labeled medium. Isolation of the protein followed the protocol described by Slijper et al. (1997), but in the presence of 5 mM of dithiothreitol (DTT). In order to produce the dimeric form, the DTT was removed during purification. The dimer was separated from the monomer by gel filtration on a Superdex 75 column (Amersham Pharmacia). The lac-SymL operator (5'-GAATTGTGAGCGCTCACAATTC-3') was purchased HPLC-purified from Carl Roth GmbH and Eurogentec. All samples were concentrated using Amicon concentrators and ultrafiltration membranes from Millipore.

H–D exchange

An aqueous sample containing 2 mM dimeric ^{15}N -labeled lacHP62 V52C mutant and 2 mM unlabeled lac-SymL operator, 10 mM H_3BO_3 , and 20 mM KCl, was used to set up the NMR experiments. The same sample was then lyophilized and afterward dissolved in D_2O to start the H–D exchange. The dead time elapsed between dissolving the sample in D_2O and recording the first spectrum was ~ 15 min. After dissolving in D_2O , the pH of the sample was adjusted to the required values (pH meter reading = 9.5) by adding NaOD. The exchange experiment was performed at 308.5 K.

NMR spectroscopy

Assignments of the backbone amide protons were taken from published data on the lacHP62-SymL complex (BMRB 4813). All NMR experiments were performed on a Bruker Avance spectrometer operating at 900 MHz. Series of ^1H – ^{15}N HSQC and homonuclear 2D NOESY spectra were simultaneously acquired as one pseudo-3D spectrum, with the third pseudo-dimension representing the time course for the H–D exchange. After acquisition of each four NOESY scans, one ^1H – ^{15}N HSQC scan was interleaved and stored in a separate memory buffer. In total, 16 NOESY and four HSQC scans were accumulated for every t_1 increment. Both interleaved 2D experiments were recorded with 800 (F2) \times 256 (F1) complex points. An interscan recovery delay of 0.69 sec was used. The 2D NOE spectra were recorded with a NOE evolution delay of 100 msec. All spectra were processed using NMRPipe (Delaglio et al. 1995). The indirect F1 dimension of the 2D NOE spectra was extended by

256 data points using linear prediction, and zero-filled to 1024 data points; FIDs were then apodized by multiplying with a squared cosine bell window function. The same window function was used in the acquisition dimension, followed by zero-filling to 2048 data points. Automatic baseline correction was applied in both dimensions. The ^1H - ^{15}N HSQC spectra were likewise processed using a squared cosine bell window function after zero-filling to 2048 (F2) and 512 (F1) points.

Data analysis

Volumes of cross-peaks in the ^1H - ^{15}N HSQC and 2D NOESY spectra were obtained using a standard integration routine in NMRView (Johnson and Blevins 1994). Their time course was fitted to a single exponential decay with three parameters (i.e., intensity at zero time elapsed, H-D decay rate, and a possible offset), using the nonlinear least-squares Levenberg-Marquardt minimization implemented in Gnuplot 3.7 (<http://www.gnuplot.info>). Errors for decay rates were taken as standard deviations from the Gnuplot fitting. Intrinsic exchange rates, k_{int} , were predicted using the program SPHERES (<http://www.fccc.edu/research/labs/roder/sphere>).

Electronic supplemental material

A figure showing H/D exchange decays and the fits to single exponential functions for all individual H^{N} signals and their mutual HN-HN NOEs.

Acknowledgments

We thank P. Gros for stimulating scientific discussions, A. George for supporting protein production, K. Houben for analysis scripts, and R. Wechselberger for support in acquiring some of the NMR spectra. R.K.S. was the recipient of a Ph.D. fellowship from CNPq (Brazil).

References

- Arrington, C.B. and Robertson, A.D. 2000. Microsecond to minute dynamics revealed by EX1-type hydrogen exchange at nearly every backbone hydrogen bond in a native protein. *J. Mol. Biol.* **296**: 1307–1317.
- Arrington, C.B., Teesch, L.M., and Robertson, A.D. 1999. Defining protein ensembles with native-state NH exchange: Kinetics of interconversion and cooperative units from combined NMR and MS analysis. *J. Mol. Biol.* **285**: 1265–1275.
- Bai, Y., Milne, J.S., Mayne, L., and Englander, S.W. 1993. Primary structure effects on peptide group hydrogen exchange. *Proteins* **17**: 75–86.
- Bai, Y., Sosnick, T.R., Mayne, L., and Englander, S.W. 1995. Protein folding intermediates: Native-state hydrogen exchange. *Science* **269**: 192–197.
- Berger, A. and Linderström-Lang, K. 1957. Deuterium exchange of poly-DL-alanine in aqueous solution. *Arch. Biochem. Biophys.* **69**: 106–118.
- Boelens, R., Gros, P., Scheek, R.M., Verpoorte, J.A., and Kaptein, R. 1985. Hydrogen exchange of individual amide protons in the *E. coli* lac repressor DNA-binding domain: A nuclear magnetic resonance study. *J. Biomol. Struct. Dyn.* **3**: 269–280.
- Cantor, C.R. and Schimmel, P. R. 1980. *Biophysical chemistry. Part III: The behavior of biological macromolecules*. W.H. Freeman, San Francisco.
- Delaglio, F., Grzesiek, S., Vuister, G.W., Zhu, G., Pfeifer, J., and Bax, A. 1995. NMRPipe: A multidimensional spectral processing system based on UNIX pipes. *J. Biomol. NMR* **6**: 277–293.
- Dempsey, C. 2001. Hydrogen exchange in peptides and proteins using NMR spectroscopy. *Prog. Nucl. Magn. Res. Sp.* **39**: 135–170.
- Englander, S.W. 2000. Protein folding intermediates and pathways studied by hydrogen exchange. *Annu. Rev. Biophys. Biomol. Struct.* **29**: 213–238.
- Englander, S.W. and Kallenbach, N.R. 1983. Hydrogen exchange and structural dynamics of proteins and nucleic acids. *Q. Rev. Biophys.* **16**: 521–655.
- Englander, S.W., Englander, J.J., McKinnie, R.E., Ackers, G.K., Turner, G.J., Westrick, J.A., and Gill, S.J. 1992. Hydrogen exchange measurement of the free energy of structural and allosteric change in hemoglobin. *Science* **256**: 1684–1687.
- Englander, S.W., Mayne, L., Bai, Y., and Sosnick, T.R. 1997. Hydrogen exchange: The modern legacy of Linderström-Lang. *Protein Sci.* **6**: 1101–1109.
- Felitsky, D.J. and Record Jr., M.T. 2003. Thermal and urea-induced unfolding of the marginally stable lac repressor DNA-binding domain: A model system for analysis of solute effects on protein processes. *Biochemistry* **42**: 2202–2217.
- Ferraro, D.M., Lazo, N.D., and Robertson, A.D. 2004. EX1 hydrogen exchange and protein folding. *Biochemistry* **43**: 587–594.
- Hare, D.L. and Sadler, J.R. 1978. Cloning of the lacI gene into a ColE1 plasmid. *Gene* **3**: 269–278.
- Hvidt, A. and Nielsen, S.O. 1966. Hydrogen exchange in proteins. *Adv. Protein Chem.* **21**: 287–386.
- Jaravine, V.A., Alexandrescu, A.T., and Grzesiek, S. 2001. Observation of the closing of individual hydrogen bonds during TFE-induced helix formation in a peptide. *Protein Sci.* **10**: 943–950.
- Johnson, B.A. and Blevins, R.A. 1994. NMRView: A computer program for the visualization and analysis of NMR data. *J. Biomol. NMR* **4**: 603–614.
- Kalodimos, C.G., Folkers, G., Boelens, R., and Kaptein, R. 2001. Strong DNA binding by covalently linked dimeric Lac headpiece: Evidence for the crucial role of the hinge helices. *Proc. Natl. Acad. Sci.* **98**: 6039–6044.
- Kalodimos, C.G., Boelens, R., and Kaptein, R. 2002. A residue-specific view of the association and dissociation pathway in protein-DNA recognition. *Nat. Struct. Biol.* **9**: 193–197.
- Kim, K. and Woodward, C. 1993. Protein internal flexibility and global stability: Effect of urea on hydrogen exchange rates of bovine pancreatic trypsin inhibitor. *Biochemistry* **32**: 9609–9613.
- Loh, S.N., Rohl, C.A., Kiefhaber, T., and Baldwin, R.L. 1996. A general two-process model describes the hydrogen exchange behavior of RnaseA in unfolding conditions. *Proc. Natl. Acad. Sci.* **93**: 1982–1987.
- Luque, I., Leavitt, S.A., and Freire, E. 2002. The linkage between protein folding and functional cooperativity: Two sides of the same coin? *Annu. Rev. Biophys. Biomol. Struct.* **31**: 235–256.
- Mayo, S.L. and Baldwin, R.L. 1993. Guanidinium chloride induction of partial unfolding in amide proton exchange in RNase A. *Science* **262**: 873–876.
- Miller, D.W. and Dill, K.A. 1995. A statistical mechanical model for hydrogen exchange in globular proteins. *Protein Sci.* **4**: 1860–1873.
- Miranker, A., Robinson, C.V., Radford, S.E., Aplin, R.T., and Dobson, C.M. 1993. Detection of transient protein folding populations by mass spectrometry. *Science* **262**: 848–849.
- Myers, J.K. and Oas, T.G. 2002. Mechanism of fast protein folding. *Annu. Rev. Biochem.* **71**: 783–815.
- Pinheiro, T.J.T., Cheng, H., Seeholzer, S.H., and Roder, H. 2000. Direct evidence for cooperative unfolding of cytochrome *c* in lipid membranes from ^1H - ^2H exchange kinetics. *J. Mol. Biol.* **303**: 617–626.
- Qian, H. and Schellman, J.A. 1992. Helix-coil theories: A comparative study for finite length polypeptides. *J. Phys. Chem.* **96**: 3987–3994.
- Qu, Y. and Bolen, D.W. 2003. Hydrogen exchange kinetics of RNase A and urea: TMAO paradigm. *Biochemistry* **42**: 5837–5849.
- Roder, H., Wagner, G., and Wüthrich, K. 1985. Amide proton exchange in proteins by EX1 kinetics: Studies of the basic pancreatic trypsin inhibitor at variable p2H and temperature. *Biochemistry* **24**: 7396–7407.
- Sadler, J.R., Sasmor, H., and Betz, J.L. 1983. A perfectly symmetric lac operator binds the lac repressor very tightly. *Proc. Natl. Acad. Sci.* **80**: 6785–6789.
- Simons, A., Tils, D., von Wilcken-Bergmann, B., and Müller-Hill, B. 1984. Possible ideal lac operator: *Escherichia coli* lac operator-like sequences from eukaryotic genomes lack the central G X C pair. *Proc. Natl. Acad. Sci.* **81**: 1624–1628.
- Sivaraman, T., Arrington, C.B., and Robertson, A.D. 2001. Kinetics of unfolding and folding from amide hydrogen exchange in native ubiquitin. *Nat. Struct. Biol.* **8**: 331–333.
- Slijper, M., Boelens, R., Davis, A.L., Konings, R.N.H., van der Marel, G.A., van Boom, J.H., and Kaptein, R. 1997. Backbone and side chain dynamics of lac repressor headpiece (1–56) and its complex with DNA. *Biochemistry* **36**: 249–254.
- Tabor, S. and Richardson, C.C. 1985. A bacteriophage T7 RNA polymerase/promoter system for controlled exclusive expression of specific genes. *Proc. Natl. Acad. Sci.* **82**: 1074–1078.
- Uchida, K., Markley, J.L., and Kainosho, M. 2005. Carbon-13 NMR method for the detection of correlated hydrogen exchange at adjacent backbone peptide

- amides and its application to hydrogen exchange in five antiparallel β strands within the hydrophobic core of *Streptomyces subtilisin inhibitor* (SSI). *Biochemistry* **44**: 11811–11820.
- Wagner, G. 1980. A novel application of nuclear Overhauser enhancement (NOE) in proteins: Analysis of correlated events in the exchange of internal labile protons. *Biochem. Biophys. Res. Commun.* **97**: 614–620.
- . 1983. Characterization of the distribution of internal motions in the basic pancreatic trypsin inhibitor using a large number of internal NMR probes. *Q. Rev. Biophys.* **16**: 1–87.
- Woodward, C., Simon, I., and Tüchsen, E. 1982. Hydrogen exchange and the dynamic structure of proteins. *Mol. Cell. Biochem.* **48**: 135–160.
- Zimm, B.H. and Bragg, J.K. 1959. Theory of the phase transition between helix and random coil in polypeptide chains. *J. Chem. Phys.* **31**: 526–535.